Phytomedicine 92 (2021) 153759

Contents lists available at ScienceDirect

Phytomedicine

journal homepage: www.elsevier.com/locate/phymed

Effective-components combination improves airway remodeling in COPD rats by suppressing M2 macrophage polarization via the inhibition of mTORC2 activity

Lan Liu [a,b,c,1], Yanqin Qin [a,b,c,1], Zehui Cai [a,b,c], Yange Tian [a,b,c], Xuefang Liu [a,b,c], Jiansheng Li [a,b,d], Peng Zhao [a,b,c,*]

[a] Henan Key Laboratory of Chinese Medicine for Respiratory Disease, Henan University of Chinese Medicine, Zhengzhou 450046, Henan Province, China
[b] Collaborative Innovation Center for Chinese Medicine and Respiratory Diseases co-constructed by Henan province & Education Ministry of P.R. China, PR China
[c] Academy of Chinese Medical Sciences, Henan University of Chinese Medicine, Zhengzhou 450046, Henan Province, China
[d] Department of Respiratory Diseases, the First Affiliated Hospital of Henan University of Chinese Medicine, Zhengzhou 450000, China

ARTICLE INFO

Keywords:
Chronic obstructive pulmonary disease
Effective-components combination
Airway remodeling
Macrophage polarization
mTORC2 signals

ABSTRACT

Background: In chronic obstructive pulmonary disease (COPD), M2 macrophages release multiple tissue repair-related factors, leading to airway remodeling, a significant pathological characteristic. Meanwhile, effective-components combination (ECC), derived from Bufei Yishen formula (BYF), is an effective treatment for COPD.
Purpose: To determine the potential mechanisms of ECC in airway remodeling in COPD by suppressing M2 macrophage polarization.
Methods: We established a rat COPD Model using exposure to cigarette smoke and bacterial infection to investigate the efficacy of ECC. We also treated macrophages with IL-4 for 12 h to explore the in vivo effect of ECC on M2 macrophage polarization and mTORC2 signals.
Results: The disease severity of COPD rats could be alleviated by ECC treatment, which improved pulmonary function and alleviated pathological injuries in lung tissue and the inflammatory cytokine levels. Meanwhile, ECC could ameliorate airway remodeling by reducing collagen deposition, hindering airway mucus hypersecretion and smooth muscle cell proliferation, and reducing the number of M2 macrophages in the lung tissues of COPD rats. Furthermore, with IL-4-induced macrophages, we found that ECC could suppress M2 macrophage polarization by decreasing the levels of M2 macrophage markers. Finally, we discovered that ECC inhibited mTORC2 activity by examining p-mTOR^{2481} and its downstream protein p-Akt^{473}.
Conclusions: ECC exerts beneficial effects on airway remodeling in COPD rats, likely by suppressing M2 macrophage polarization via the inhibition of mTORC2 activity.

Introduction

Chronic obstructive pulmonary disease (COPD) is a common, preventable, and treatable disease that is also progressive and often irreversible (Global Initiative for Chronic Obstructive Lung Disease 2021). Owing to its high morbidity and mortality, COPD has been the third leading cause of death worldwide (Lortet-Tieulent et al., 2019). Airway remodeling is a process involving multiple pathological changes, including collagen deposition, peribronchial fibrosis, and hyperplasia of airway epithelial cells (Hirota and Martin, 2013), leading to almost irreversible airway obstruction and a subsequent decrease in lung function (Hogg et al., 2004). Bronchodilators and glucocorticosteroids are usually used to treat airway remodeling. However, they can only decrease the severity of the disease and improve the patients' quality of

Abbreviations: APL, Aminophylline; AQP5, Aquaporin 5; Arg-1, Arginase-1; bFGF, Basic fibroblast growth factor; COPD, Chronic obstructive pulmonary disease; ECC, Effective-component combination; FRC, Functional residual capacity; IRF4, Interferon regulatory factor 4; MAN, Mean alveolar number; MLI, Mean linear intercept; MUC5AC, mucin 5AC; PDGF-A, Platelet-derived growth factor A; PEF, Peak expiratory flow; TGF-β, Transforming growth factor-β; VT, Tidal volume; α-SMA, α-smooth muscle actin.

* Corresponding author at: 156 Jinshui Dong road, Zhengzhou Henan 450046, China.
E-mail address: zhaopeng871@126.com (P. Zhao).

[1] These authors contributed equally to this work.

https://doi.org/10.1016/j.phymed.2021.153759
Received 8 June 2021; Received in revised form 22 August 2021; Accepted 12 September 2021
Available online 13 September 2021

Table 1
Primer sequences for real-time PCR.

Gene	Forward primer (5′–3′)	Reverse primer (5′–3′)
Arg-1	TGTCCCTAATGACAGCTCCTT	GCATCCACCCAAATGACACAT
IRF4	AAAGGCAAGTTCCGAGAAGGG	CTCGACCAATTCCTCAAAGTCA
KLF4	GTGCCCCGACTAACCGTTG	GTCGTTGAACTCCTCGGTCT
PDGFA	TGGCTCGAAGTCAGATCCACA	TTCTCGGGCACATGGTTAATG
TGF-β	CTCCCGTGGCTTCTAGTGC	GCCTTAGTTTGGACAGGATCTG
CTGF	GACCCAACTATGATGCGAGCC	CCCATCCCACAGGTCTTAGAAC
GAPDH	AGGTCGGTGTGAACGGATTTG	GGGGTCGTTGATGGCAACA

life, and they are ineffective in slowing down the development of lung injury and airway remodeling (Jones et al., 2016; Tashkin et al., 2008). Therefore, it is necessary to develop new drugs for airway remodeling in COPD.

Noxious particles or gas exposure can recruit inflammatory cells, such as dendritic cells and macrophages, causing chronic airway inflammation and tissue remodeling in COPD patients. Two types of polarized macrophages, classically activated (M1) or activated (M2), play various critical roles in chronic inflammation and abnormal tissue repair in COPD (Parisi et al., 2018). M1 macrophages, induced by Th1 cytokines, produce a large amount pro-inflammatory cytokines to participate in the inflammatory response (Yamasaki and Eeden, 2018). On the contrary, M2 macrophages, induced by Th2 cytokines, overexpress arginase-1 (Arg-1), interferon regulatory factor 4 (IRF4) and the mannose receptor CD206 (Mrc1) and release transforming growth factor-β (TGF-β) (Hou et al., 2018; Mills et al., 2000), resulting in myofibroblast activation, smooth muscle hyperplasia, and abnormal tissue repair (Shaykhiev et al., 2009). Thus, M2 macrophages play a crucial role in the airway remodeling of COPD (Vlahos and Bozinovski, 2014).

The generation of M2 macrophages is affected by mTOR signaling. The mechanistic target of rapamycin (mTOR) senses and integrates environmental factors to mediate cell metabolism, survival, aging, and growth. The mTOR signal is composed of mTOR complex 1 (mTORC1) and mTOR complex 2 (mTORC2) (Zeng et al., 2016). mTORC1, which typically phosphorylates p70 S6 kinase (S6K), is crucial for the differentiation of T cells into Th1/Th17 cells. By contrast, mTORC2 typically phosphorylates Akt at serine 473, playing a crucial part in Th2 cell differentiation (Linke et al., 2017). In addition, blocking mTORC2 can reduce the generation of M2 macrophages (Hallowell et al., 2017). Moreover, mTORC2 activation can increase the metabolism of M2 macrophages (Huang et al., 2016). Therefore, we hypothesized that mTORC2 activation-mediated M2 macrophage polarization contributed to airway remodeling in COPD.

On the other hand, the Bufei Yishen formula (BYF) (Patent ZL.201110117578.1), composed of 12 Chinese medicines, is effective in improving clinical symptoms, reducing the frequency of acute episodes, and improving the quality of life of patients with stable COPD (SY Li et al., 2012). In addition, BYF has beneficial effects on COPD rats by decreasing inflammatory responses, improving airway remodeling, and reducing pulmonary pathological impairment (Li et al., 2014). However, thousands of compounds in the 12 Chinese herbal drugs that make up BYF make it difficult to identify the active substances in BYF or delineate the mechanism of BYF. Thus, five active compounds, including nobiletin, paeonol, icariin, 20-S-ginsenoside Rh1, and astragaloside IV, were identified in BYF and combined into an effective-components combination (ECC), the bioactive equivalent of BYF on COPD rats (Li et al., 2020). However, the mechanism of ECC remains unclear.

Here, we established the COPD Model in rats to observe the effects of ECC on the M2 macrophages in the lung tissue and airway remodeling in COPD. In addition, the underlying mechanisms of ECC in regulating M2 macrophage polarization by inhibiting mTORC2 signals were explored *in vitro*.

Materials and methods

Animals and chemicals

Forty-eight Sprague-Dawley rats (Laboratory Animal Center of Henan Province, Zhengzhou, China) were used. All procedures were approved by the First Affiliated Hospital, Henan University of Traditional Chinese Medicine in Zhengzhou, China (Batch number: DWLL202003210; March 30, 2020).

ECC consisted of 12.5 mg/ml 20-S-ginsenoside Rh1 (PubChem CID: 1285592), 2.5 mg/ml astragaloside IV (PubChem CID: 13943297), 50 mg/ml icariin (PubChem CID: 5318997), 2 mg/ml nobiletin (PubChem CID: 72,344), and 3.125 mg/ml paeonol (PubChem CID: 11092) (Chengdu Must BioTech Co., Ltd., Chengdu, China). The purity of all compounds was more than 98%. The rat interleukin-6 (IL-6) (ERC003), IL-1β (ERC007), and TNF-α (ERC102a) enzyme-linked immunosorbent assay (ELISA) kits were from Neobioscience (Shenzhen, China). Rat MMP-9, TIMP-1, and VEGF were examined using various ELISA kits (Boster, Wuhan, China). Rat MMP-12, COL-I, COL-III, and bFGF were examined using specific ELISA kits (Elabscience Biotechnology, Wuhan, China). Finally, rat AQP5 and MUC5AC were detected in the BALF using ELISA kits (Cusabio Biotech Co., Ltd., Wuhan, China).

COPD Model preparation and administration

The animals were randomly divided into four groups: Normal, Model, ECC, and APL, with 12 animals per group. From week 1 to 8, the COPD Model animals were stimulated by tobacco smoke at 3000 ± 500 ppm for 40 min and administered with 0.1 ml of *Klebsiella pneumoniae* at 6×10^8 CFU/ml to both nostrils alternately. The Normal animals received saline instead of the bacterial solution (Li et al., 2012b). From week 9 to 16, the Normal and Model groups were intragastrically administrated with Normal saline, whereas the ECC and APL groups were intragastrically administered with 5.5 mg/kg/d ECC and 54 mg/kg/d aminophylline (APL) suspensions, respectively. The lung tissue samples were harvested at the end of week 16.

Cell culture

The mouse-derived alveolar macrophages, MH-S cells (Procell, Wuhan, China), were cultured at 37 °C, 5% CO_2, and 95% humidified air. Macrophages were treated with 35.0625 or 70.125 μg/ml ECC or 0.1% dimethyl sulfoxide for 3 h and stimulated by 20 ng/ml IL-4 for 12 h. Then, samples were harvested.

Pulmonary function analysis

We measured the tidal volume (V_T), minute volume (MV), peak expiratory flow (PEF), and expiratory flow at 50% tidal volume (EF50) using unrestrained pulmonary function plethysmography. On the other hand, functional residual capacity (FRC), forced expiratory volume at 0.1 s (FEV 0.1), and forced vital capacity (FVC) were detected at the end of week 16.

Histopathology

The lung tissue slices were stained with hematoxylin–eosin (HE), AB-PAS, or Masson's trichrome (Servicebio, Wuhan, China) and observed using optical microscopy (Olympus, Tokyo, Japan). The mean alveolar number (MAN) and mean linear intercept (MLI) of the lung sections were counted using Adobe Photoshop CC. IPP 6.0 was used to examine collagen volume fraction.

Immunohistochemistry

The lung slices were covered with 3% BSA for 30 min and incubated

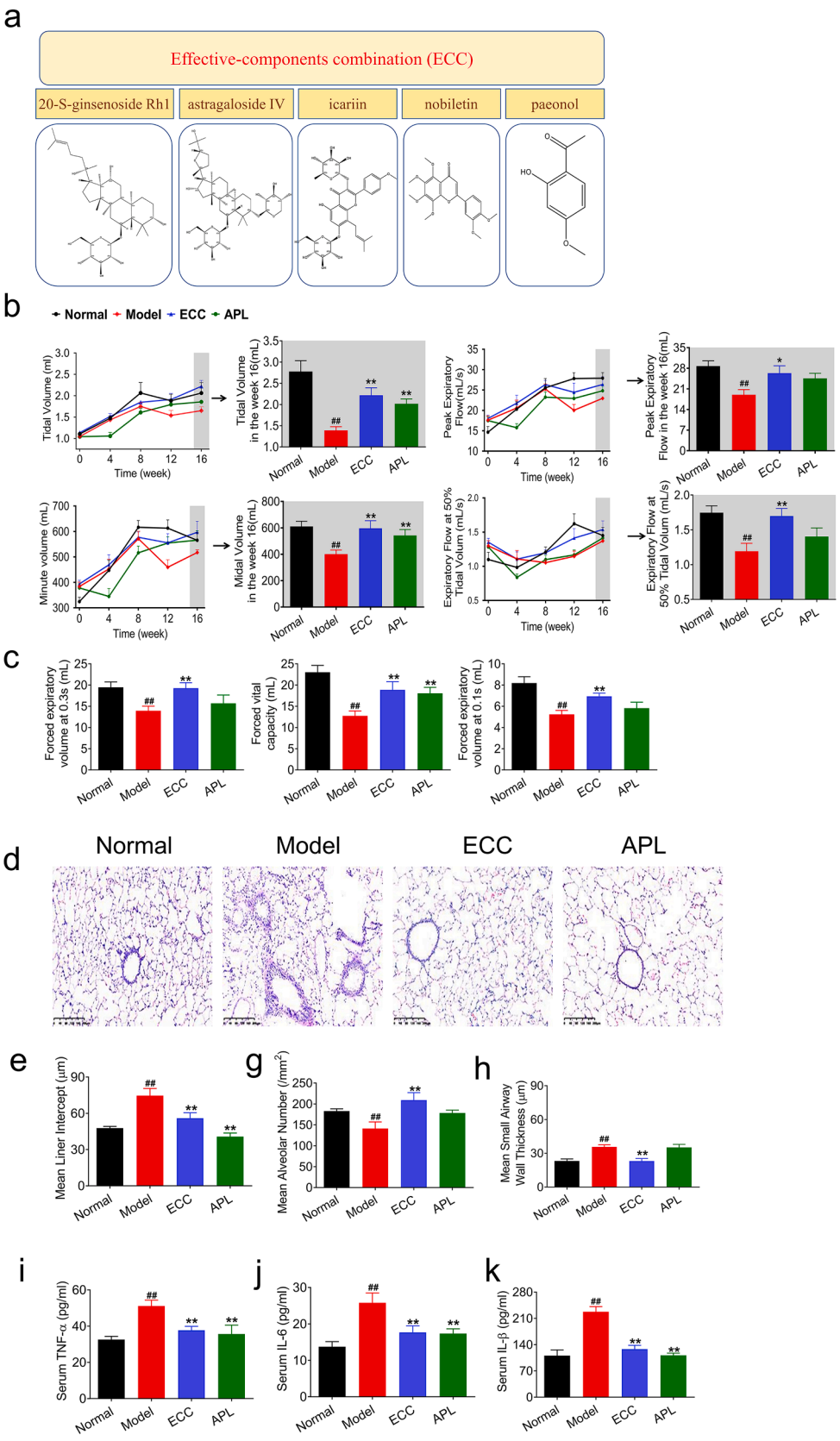

Fig. 1. Effective-components combination (ECC) effectively improved severity of COPD. (a): the chemical structure of ECC compounds. (b): the tidal volume (V_T), minute volume (MV), peak expiratory flow (PEF) and expiratory flow at 50% tidal volume (EF50). (c): the functional residual capacity (FRC), forced vital capacity (FVC), and forced expiratory volume at 0.1 s (FEV 0.1). (d): HE staining of lung tissue in rats (200 ×). (e): Mean linear intercept (MLI). (f) Mean alveolar number (MAN). (g): Mean small airway wall thickness. (h), (i), (j): The levels of IL-6, IL-1β and TNF-α in the serum. All data showed as the mean ± SEM (n = 6). $^{\#}$ $p < 0.05$, $^{\#\#}$ $p < 0.01$, *vs.* Normal group; * $p < 0.05$, ** $p < 0.01$, *vs.* Model group.

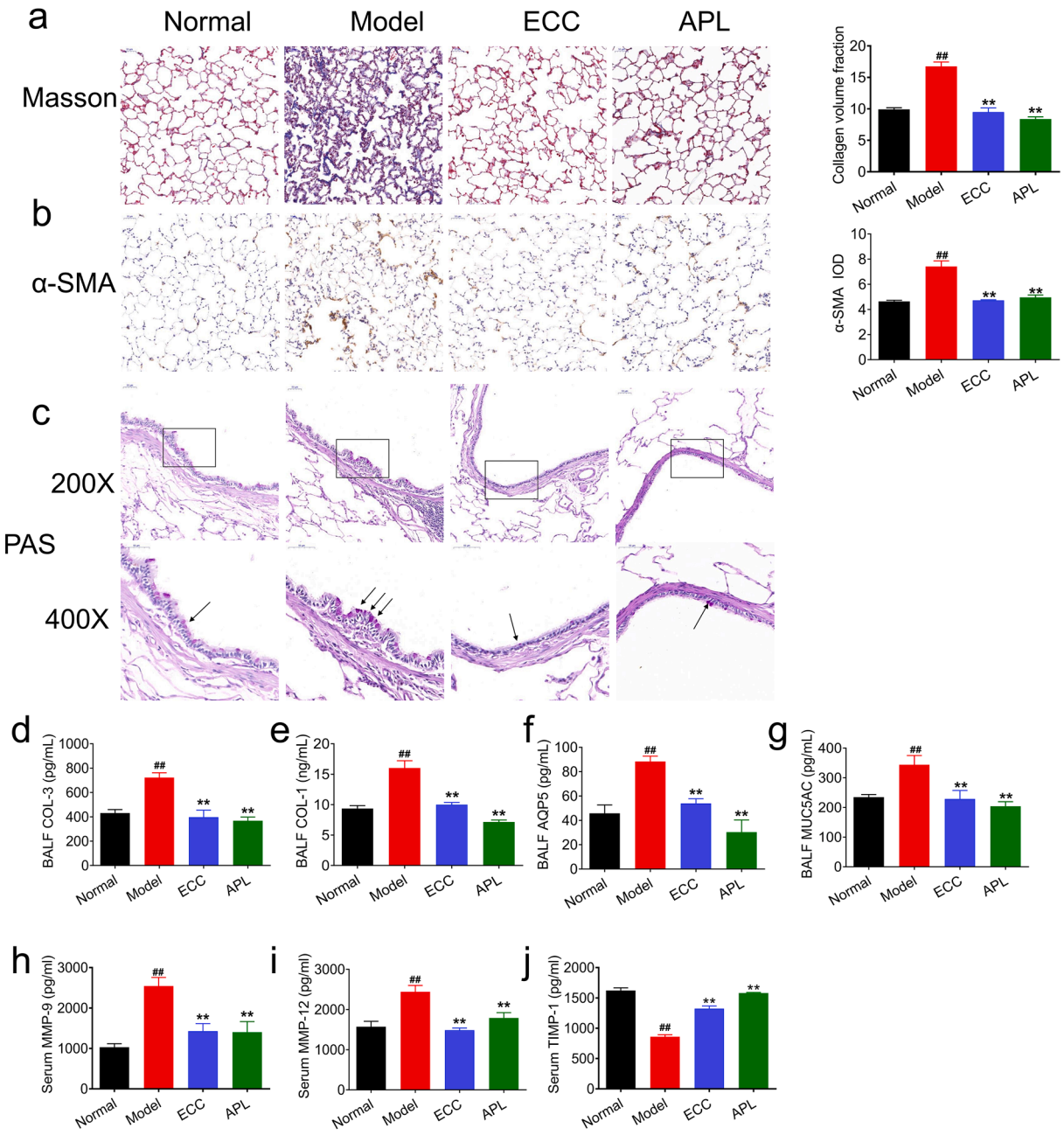

Fig. 2. Effective-components combination (ECC) alleviated airway remodeling on COPD. (a): Masson staining (magnification, 200 ×) and collagen volume fraction. (b): Expression level of α-Smooth muscle actin (α-SMA) (200 ×) and the integral optical density (IOD) of α-SMA. (c): AB-PAS staining imagines of the airway (200 ×, 400 ×). (d), (e): Level of Collagen 3 (COL-3) and Collagen 1 (COL-1) in the bronchoalveolar lavage fluid (BALF). (f), (g): Expression levels of mucin 5AC (MUC5AC) and recombinant aquaporin 5 (AQP5) in the BALF. (h), (i), (j): Levels of MMP-9, TIMP-1 and MMP-12 in the serum. All data showed as the mean ± SEM ($n = 6$). $^{\#}$ $p < 0.05$, $^{\#\#}$ $p < 0.01$, *vs.* Normal group; * $p < 0.05$, ** $p < 0.01$ *vs.* Model group.

with the anti-α-SMA, anti-CD68, or anti-CD206 antibodies using the DAB solution (Servicebio, Wuhan, China). In addition, integral optical density was detected using IPP 6.0.

Immunofluorescence

The cells plated in 15-mm confocal dishes (Biosharp, Beijing, China) for 24 h were treated with ECC and IL-4 for 12 h. Then, they were fixed with 4% formaldehyde for 15 min, permeabilized with 0.3% Triton X-100 for 30 min, and blocked with the blocking buffer for 2 h. Next, the cells were incubated with the primary Arg-1, CD206, TGF-β, p-Akt^{473}, p-mTOR^{2481}, p-STAT6, p-STAT3, or CTGF antibodies overnight at 4 °C, with corresponding secondary antibodies for 2 h, counterstained with DAPI for 2 min, and mounted in the antifade mounting medium.

Western blotting

The cells were lysed on ice using a protein extraction kit. First, we measured the protein concentration. Next, the denatured protein was subjected to electrophoresis and blotted onto polyvinylidene difluoride membranes. After blocking with 5% non-fat milk in 1 × TBST, membranes were incubated with the primary antibodies at 4 °C overnight and the corresponding secondary antibodies. Then, we detected the protein bands using the ECL reagent.

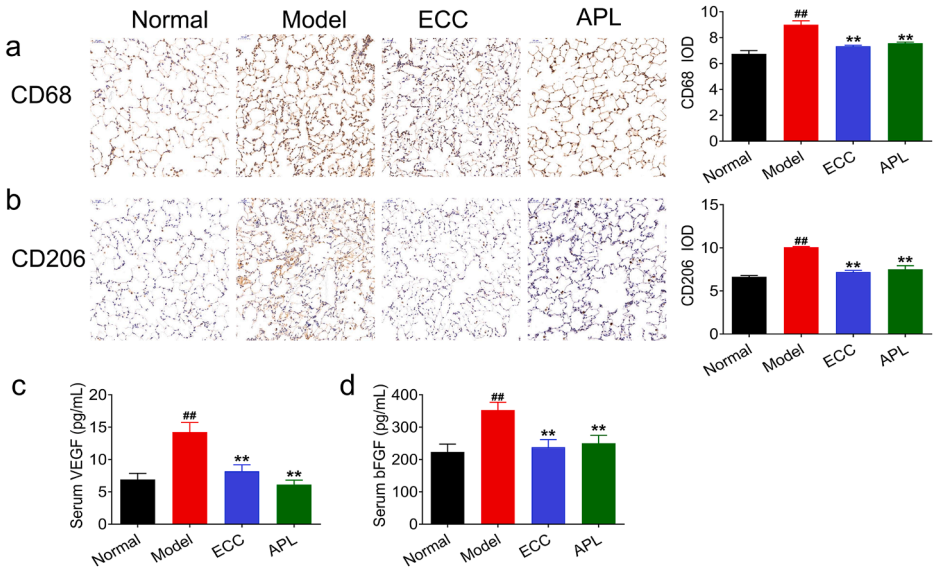

Fig. 3. Effective-components combination (ECC) reduced the quantity of macrophages and M2 macrophages and suppressed the expression of tissue repair-related factors on COPD. (a), (b): the levels of CD68 (200 ×) and CD206 (200 ×), and the integral optical density (IOD) of CD68 and CD206. (c), (d): Level of VEGF and bFGF in the serum. All data showed as the mean ± SEM ($n = 6$). $^{\#}$ $p < 0.05$, $^{\#\#}$ $p < 0.01$, *vs.* Normal group; * $p < 0.05$, ** $p < 0.01$, *vs.* Model group.

RNA extraction and PCR

Total RNA was obtained from MH-S cells using the TRIZOL reagent (Invitrogen, Carlsbad, CA, USA). cDNA was synthesized using the HiScript II Q RT SuperMix (Vazyme, Nanjing, China) with 1 μg of RNA. Real-time PCR reactions were conducted using ChamQ Universal SYBR (Vazyme, Nanjing, China) and specific primers (Table 1) in an Applied Biosystems 7500 instrument (AB, CA, USA).

Statistical analysis

SPSS 26.0 was used to analyze all data. All data were presented as mean ± SEM. The significances between the means of different groups were assessed using a one-Way ANOVA. The differences were considered statistically significant when p-values < 0.05.

Results

ECC ameliorated disease severity of COPD rats

Testing pulmonary function is the basis of diagnosing COPD. In addition, histopathological changes and inflammatory responses are important characteristics of COPD. Therefore, we investigated the effects of ECC on COPD rats by comparing the pulmonary function, pathological changes, and inflammatory cytokine levels in the ECC-treated rats to those in the untreated ones.

FRC, FVC, FEV 0.1, V_T, MV, PEF, and EF50 of the Model rats with induced COPD were reduced compared to those in the Normal rats, whereas those in the COPD rats treated with ECC or APL were increased (Fig. 1b–c). Compared to the Normal rats, the lung tissues in the Model rats showed severe pathological injuries, including increased mean linear intercept, increased mean small airway wall thickness, and decreased mean alveolar number (Fig. 1d–h). These changes in the ECC and APL-treated rats were obviously ameliorated. Additionally, the increased levels of tumor necrosis factor-α (TNF-α), IL-6, and IL-1β were reversed by ECC treatment (Fig. 1i–k). These results indicated that ECC could ameliorate the disease severity of COPD rats by improving pulmonary function, alleviating pathological injuries, and inhibiting the activation of pro-inflammatory cytokines.

ECC improved airway remodeling in COPD rats

Airway remodeling, a significant structural change in COPD, is related to reduced pulmonary function. Thus, we determined whether ECC could prevent airway remodeling by comparing the extent of collagen deposition, airway mucus hypersecretion, and the increase in smooth muscle mass in the various groups of rats.

Notably, goblet cell hyperplasia, collagen accumulation, and smooth muscle mass were increased in the lung tissues of the COPD rats and were reduced in those in the rats with COPD treated with ECC or APL (Fig. 2a–g). In addition, the protein levels of MMP-9 and MMP-12 were considerably decreased in the ECC and APL-treated rats (Fig. 2h–j). Moreover, the reduction in the TIMP-1 level was suppressed by ECC and APL treatment. These results demonstrated that ECC could alleviate airway remodeling by inhibiting goblet cell metaplasia, collagen deposition, and airway mucus obstruction and by improving the protease–antiprotease imbalance.

ECC reduced the number of M2 macrophages in the lung of COPD rats

M2 macrophages are closely associated with lung tissue remodeling and fibrosis by releasing tissue repair-related factors, including VEGF and bFGF. We determined the phenotype of the macrophages in Model rats by examining the levels of CD68 and CD206. ECC and APL could effectively reduce the number of macrophages and M2 macrophages compared to those in the Model rats (Fig. 3a–b). Furthermore, the increased levels of VEGF and bFGF in the serum of the Model rats were markedly reversed by ECC and APL treatments (Fig. 3c–d). These results showed that ECC treatment reduced the total number of macrophages and M2 macrophages in lung tissue and lowered the levels of airway remodeling-related growth factors.

ECC suppressed IL-4-induced polarization of M2 macrophages

We further explored the mechanism of ECC on M2 macrophage polarization. The levels of Arg-1 and CD206 in cells stimulated by IL-4 for 12 h were higher than those in the untreated cells, whereas ECC treatment substantially inhibited the increase of the same proteins (Fig. 4a–c). The IL-4-induced upregulated expression of IRF4 and KLF4 and the elevated levels of p-STAT3 and p-STAT6 were clearly inhibited

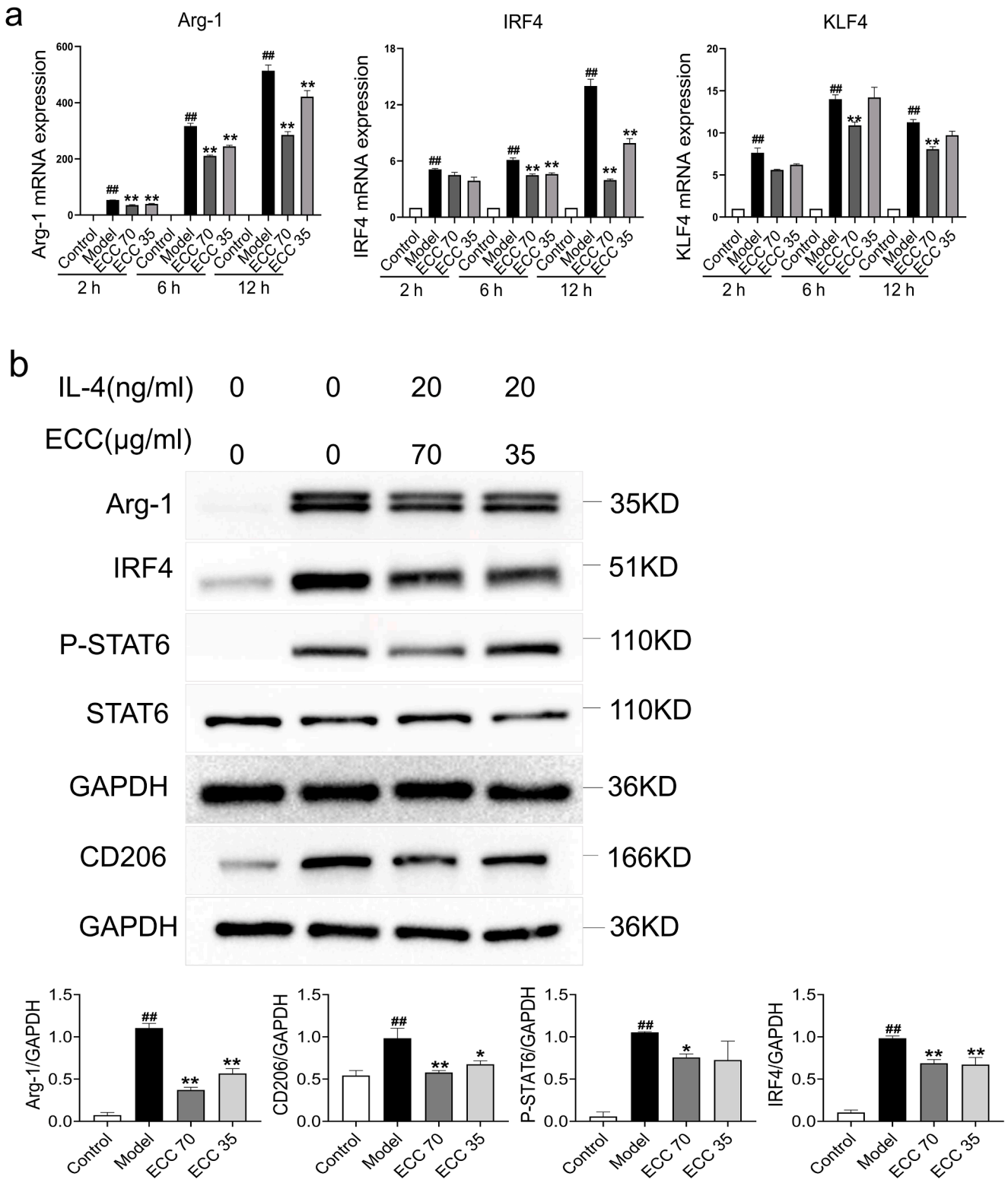

Fig. 4. Effective-components combination (ECC) inhibited M2 macrophage polarization stimulated by IL-4. (a): the mRNA expression of arginase-1 (Arg-1), *IRF4* and *KLF4* in MH-S cells. Values showed as the mean ± SEM ($n = 3$). (b): the levels of Arg-1, CD206, IRF4, p-STAT6, and STAT6 in MH-S cells using western blot. Values showed as the mean ± SEM ($n = 3$). (c): protein levels of Arg-1, CD206, p-STAT6, and p-STAT3 using immunofluorescence (400 ×). Values showed as the mean ± SEM ($n = 9$). $^{\#}p < 0.05$, $^{\#\#}p < 0.01$, *vs.* Control group; $^{*}p < 0.05$, $^{**}p < 0.01$, *vs.* Model group.

by ECC treatment (Fig. 4a–c). The mRNA levels of TGF-β, platelet-derived growth factor (PDGF-A), and CTGF were evidently overexpressed by IL-4 stimulation and had a significant reduction in ECC-treated macrophages at 12 h (Fig. 5a). Similarly, the treatment with ECC inhibited TGF-β and CTGF activation (Fig. 5b–c). Thus, ECC could inhibit M2 macrophage polarization and weaken the release of key

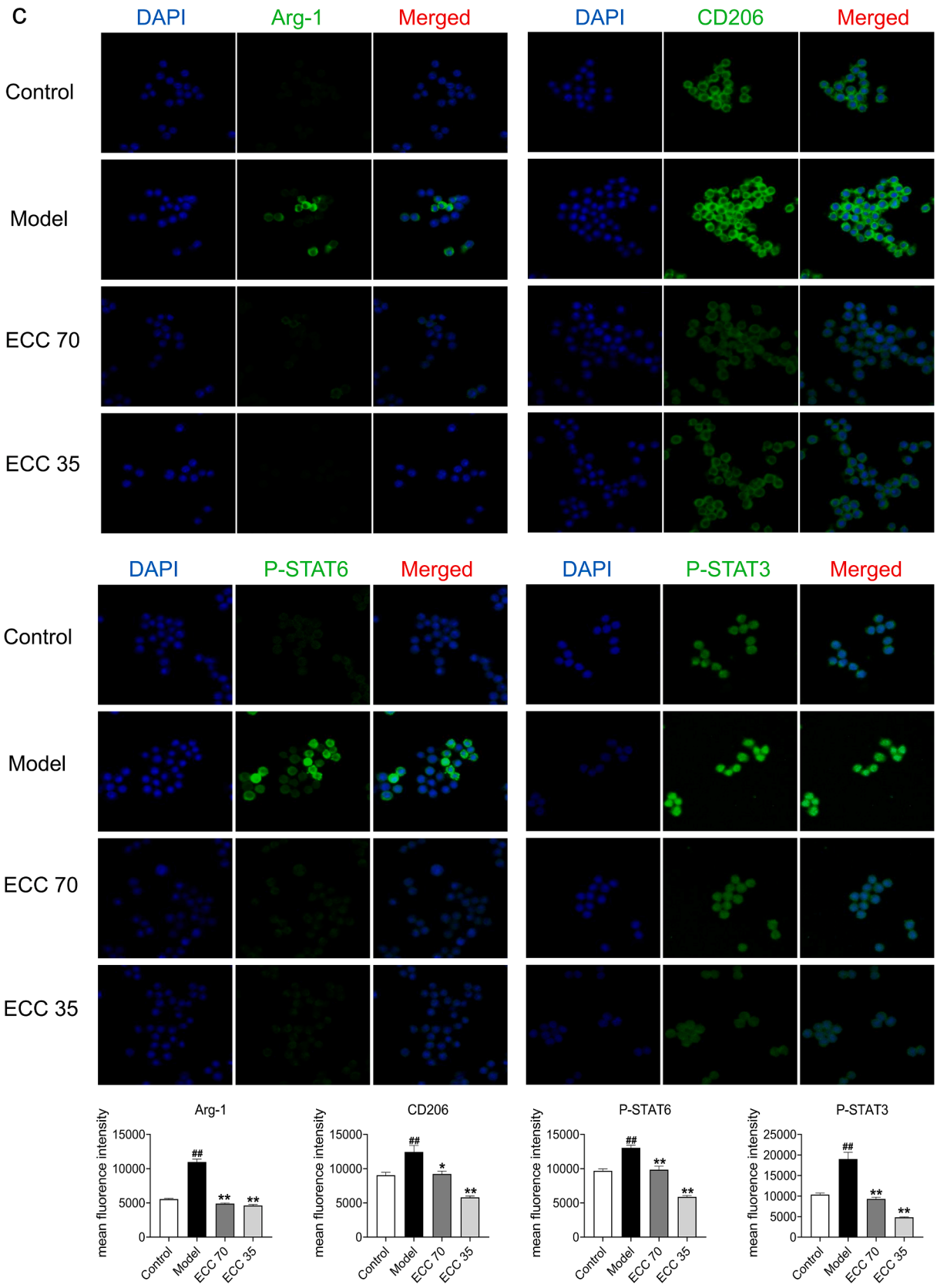

Fig. 4. (*continued*).

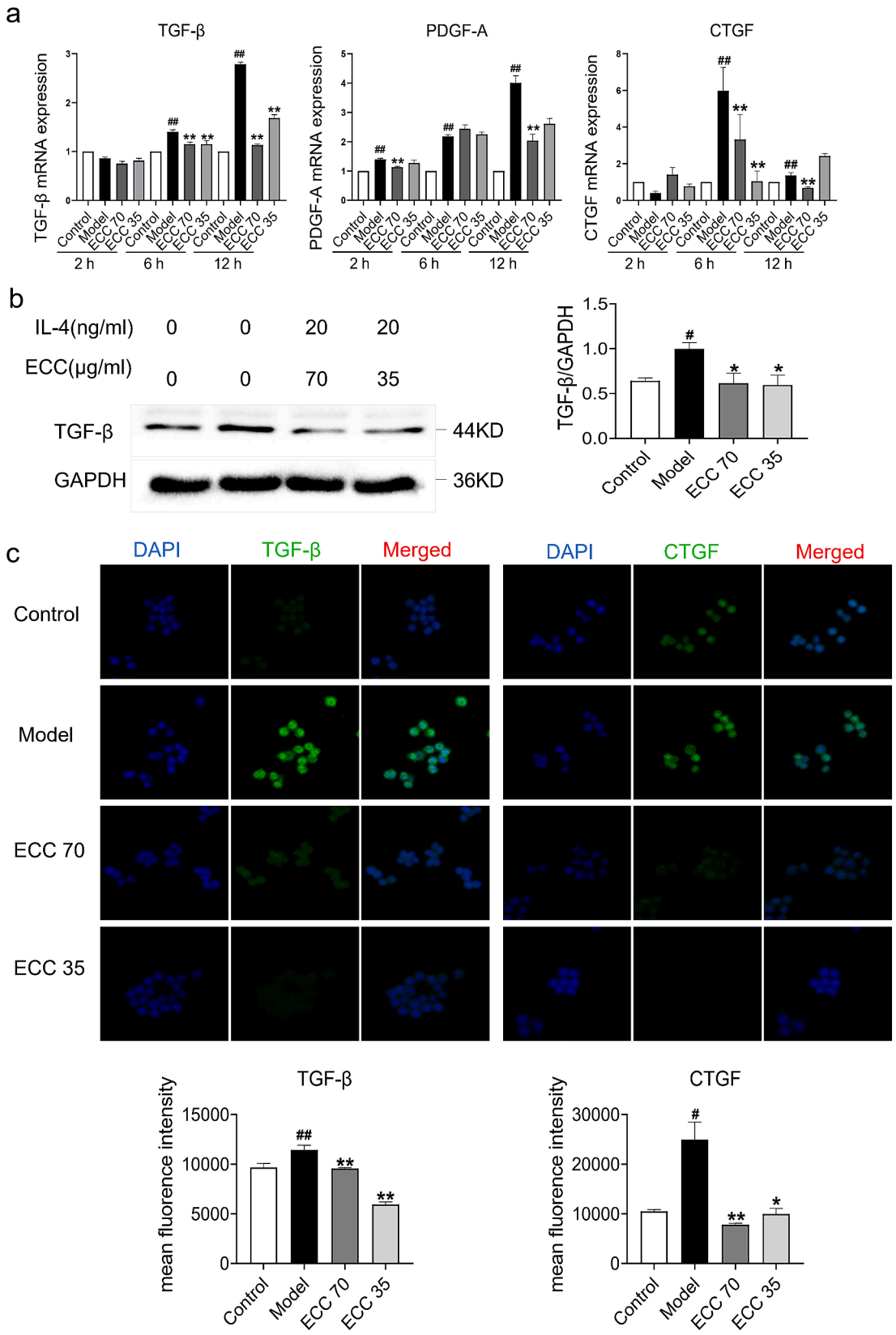

Fig. 5. Effective-components combination (ECC) weakened the release of key profibrotic factors. (a): the mRNA levels of TGF-β, PDGF-A, and CTGF in MH-S cells. Values showed as mean ± SEM ($n = 3$). (b): the expression levels of TGF-β in MH-S cells using western blot. Values showed as mean ± SEM ($n = 3$). (c): protein levels of TGF-β and CTGF using immunofluorescence (400 ×). Values showed as mean ± SEM ($n = 9$). $^{\#}p < 0.05$, $^{\#\#}p < 0.01$ *vs.* Control group; $^{*}p < 0.05$, $^{**}p < 0.01$, *vs.* Model group.

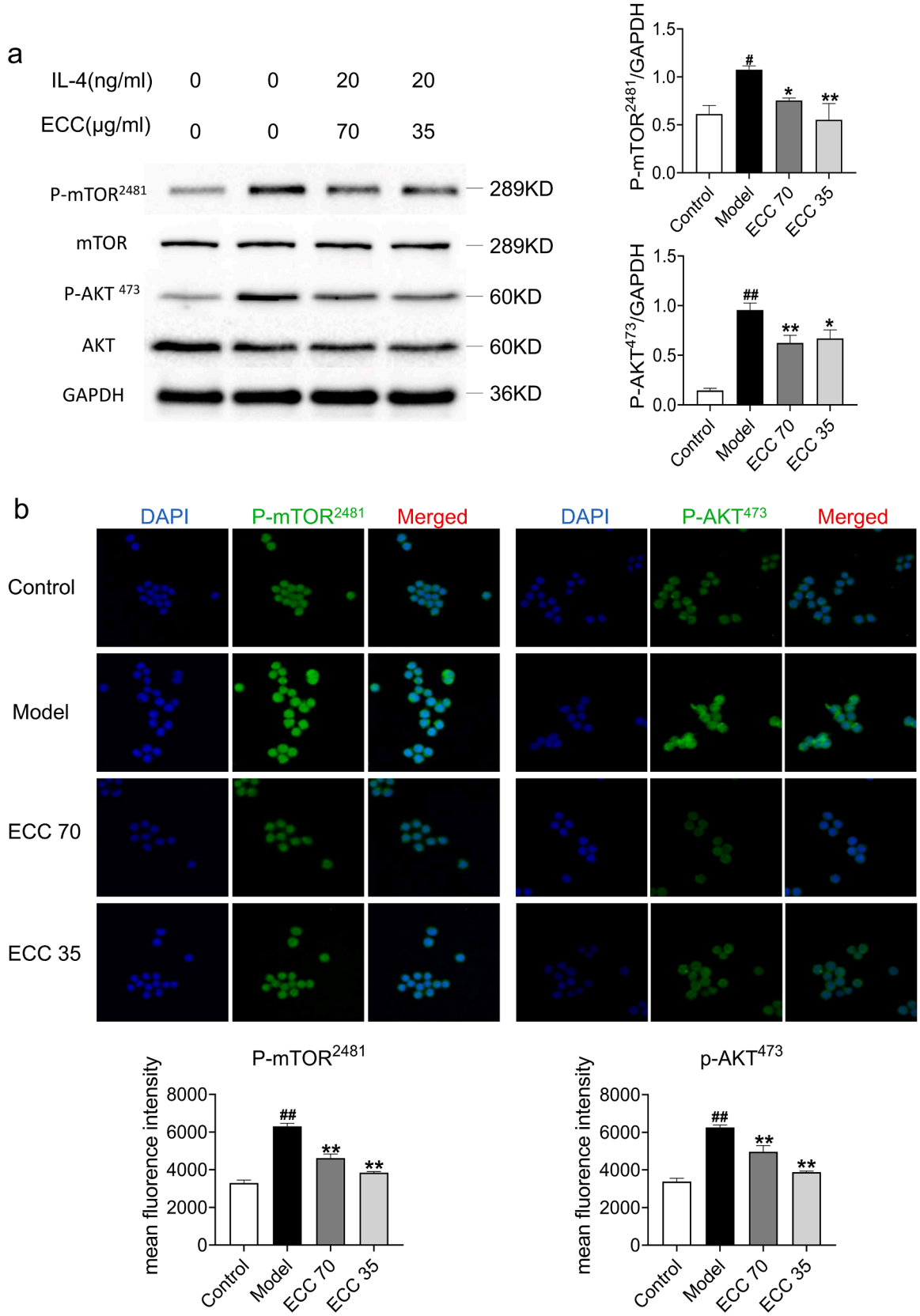

Fig. 6. Effective-components combination (ECC) suppressed the mTORC2 activation. (a): the levels of p-mTOR^{2481} and p-Akt^{473} using western blot. Values showed as mean ± SEM ($n = 3$). (b) the expression of p-mTOR^{2481} and p-Akt^{473} using immunofluorescence (400 ×). Values showed as mean ± SEM ($n = 9$). $^{\#}$ $p < 0.05$, $^{\#\#}$ $p < 0.01$ *vs*. Control group; * $p < 0.05$, ** $p < 0.01$, *vs*. Model group.

profibrotic factors.

ECC inhibited M2 macrophage polarization by inhibition of mTORC2 signaling

mTORC2 activation plays a vital role in promoting M2 macrophage polarization through Akt activation. On the other hand, Akt overexpression also leads to an enhanced expression of M2 marker genes. We determined whether ECC inhibited M2 macrophage polarization via mTORC2 signaling by analyzing the key mTORC2 marker, p-mTOR^{2481}, and a downstream target, p-Akt^{473}. We found that ECC clearly suppressed the IL-4-induced phosphorylation of mTOR at Ser 2481 (Fig. 6). In addition, mTORC2 activation could be measured by the phosphorylation status of Akt. The level of p-Akt^{473} was apparently increased in IL-4-induced cells but significantly weakened by the ECC treatment. These data revealed that ECC suppressed mTORC2 activation.

Discussion

Airway remodeling is associated with the reduction of lung function, an important pathological feature of COPD. Bronchodilators and glucocorticosteroids generally are used to improve airway remodeling by ameliorating bronchoconstriction and airway inflammation. However, they do not reverse the progress of lung injury and airway remodeling. This study confirmed that ECC could effectively improve airway remodeling and reduce the quantity of M2 macrophages in COPD rats. Furthermore, ECC could suppress M2 macrophage polarization by inhibiting mTORC2 signals.

In recent years, traditional Chinese medicines, such as BYF, have demonstrated efficacy in improving the quality of life and clinical symptoms in patients with stable COPD (SY Li et al., 2012). However, BYF's complex composition and variation of components have made it challenging to explain its underlying mechanisms. The ECC is derived from five components of BYF, including 20-S-ginsenoside Rh1, astragaloside IV, icariin, nobiletin, and paeonol. We previously used the method of effective-component compatibility to identify the pivotal active compounds from BYF, finally identifying the optimum ratio of the ECC of the five components (Li et al., 2014).

Here, we first investigated the efficacy of ECC on COPD rats. We found that ECC could improve pulmonary function, alleviate pathological damages, and reduce the inflammatory response. However, collagen deposition, increased mucin and smooth muscle mass, hyperplasia of goblet cells, and abnormal MMPs trigger extracellular matrix deposition, airway mucus hypersecretion, and lung fibroblasts activation, accelerating small airway obstruction and airway hyperreactivity and further exacerbating airway remodeling (Lai et al., 2018). Moreover, epithelial cells release a large amount of growth factors linked to airway remodeling in response to extraneous stimuli such as smoke particles. For example, an antithymic stromal lymphopoietin antibody can restrain airway remodeling by reducing the levels of MMP-9 and CTGF (Lin et al., 2019). Thus, we demonstrated that ECC suppressed airway remodeling by reducing collagen, airway mucus, MMPs, and the related growth factors, including VEGF and bFGF.

The quantity of macrophages is prominently elevated in the airways of COPD patients (Arora et al., 2018). Macrophages of distinct phenotypes can play different roles in the development of COPD. M1 macrophages achieve antimicrobial and cytotoxic effects by releasing pro-inflammatory cytokines. Meanwhile, M2 macrophages, characterized by an excessive production of CD206, TGF-β, and Arg-1, have anti-inflammatory properties relevant in tissue remodeling and repair (Xue et al., 2015). The proportion of M2/M1 phenotypes is increased in COPD patients. p-STAT6 and p-STAT3 are master regulators that induce M2 macrophage activation (Choi et al., 2016). KLF4 and IRF4 are key transcriptional factors in M2 macrophages, and their levels are distinctly increased (Liao et al., 2011).

In this study, we discovered that ECC reduced the number of macrophages and M2 macrophages in lung tissues of patients with COPD. Additionally, the expression of Arg-1 and CD206 was lowered by ECC. Meanwhile, we observed that the expression of IRF4 and KLF4 and the levels of p-STAT3 and p-STAT6 were restrained by ECC. Hence, ECC could suppress M2 macrophage polarization by inhibiting M2-related signaling proteins and transcription factors.

On the other hand, TGF-β released by M2 macrophages can induce the activation of fibroblasts, leading to the abnormal deposition of extracellular matrix (Murray et al., 2011). Furthermore, CTGF, a matricellular protein, is a vital regulator of airway remodeling, and blocking CTGF can alleviate pulmonary remodeling (Bickelhaupt et al., 2017). Meanwhile, PDGF-A can mediate airway remodeling by promoting lung fibroblasts proliferation and procollagen I synthesis (Kardas et al., 2020). Thus, ECC can control the expression of the genes encoding airway remodeling-related growth factors TGF-β, CTGF, and PDGF-A.

Finally, mTOR signals consist of two distinct complexes, namely, mTORC1 and mTORC2. mTORC2 plays a critical role in controlling M2 macrophage differentiation and the selective degradation of the adaptor proteins that suppress M2 differentiation (Hallowell et al., 2017). The phosphorylation of Akt at position 473 is the effector substrate of mTORC2 and a key mediator of M2 macrophage polarization. The enhancement of mTORC2 activation fails to promote macrophages to polarize into M2 macrophages when Akt activation is restrained (Smyth et al., 2008). Here, ECC was found to suppress mTORC2. Thus, ECC inhibits mTORC2 activity by reducing the levels of p-mTOR^{2481} and downstream protein p-Akt^{473}.

Conclusions

Our data suggest that ECC can improve COPD symptoms and airway remodeling by suppressing the mTORC2 signaling, thereby inhibiting M2 macrophage polarization and decreasing the release of fibrogenic factors.

Author contributions

Lan Liu, Yanqin Qin, and Zehui Cai performed and analyzed experiments. Yange Tian and Xuefang Liu were involved in data analysis. Peng Zhao, and Jiansheng Li designed the outline of the whole experiment. All data were generated in-house, and no paper mill was used. All authors agree to be accountable for all aspects of work ensuring integrity and accuracy.

Declaration of Competing Interest

The authors vetify that there are no known conflicts of interest concerned with this article.

Funding

This study was supported by the National Natural Science Fund of China (No. 81603473, 81973822), Young Elite Scientists Sponsorship Program by CACM (2019-QNRC2-B03), Foundation of Department of Science and Technology of HeNan Province (212102310356) and Foundation of overseas researcher.

References

Arora, S., Dev, K., Agarwal, B., Das, P., Syed, M.A., 2018. Macrophages: their role, activation and polarization in pulmonary diseases. Immunobiology 223, 383–396.

Bickelhaupt, S., Erbel, C., Timke, C., Wirkner, U., Dadrich, M., Flechsig, P., Tietz, A., Pföhler, J., Gross, W., Peschke, P., Hoeltgen, L., Katus, H.A., Gröne, H.J., Nicolay, N. H., Saffrich, R., Debus, J., Sternlicht, M.D., Seeley, T.W., Lipson, K.E., Huber, P.E., 2017. Effects of CTGF blockade on attenuation and reversal of radiation-induced pulmonary fibrosis. J. Natl. Cancer Inst. 109.

Choi, J.W., Kwon, M.J., Kim, I.H., Kim, Y.M., Lee, M.K., Nam, T.J., 2016. Pyropia yezoensis glycoprotein promotes the M1 to M2 macrophage phenotypic switch via the STAT3 and STAT6 transcription factors. Int. J. Mol. Med. 38, 666–674.
Global Initiative for Chronic Obstructive Lung Disease, 2021 report [Online], 2021, http://www.goldcopd.org.
Hallowell, R.W., Collins, S.L., Craig, J.M., Zhang, Y., Oh, M., Illei, P.B., Chan-Li, Y., Vigeland, C.L., Mitzner, W., Scott, A.L., Powell, J.D., Horton, M.R., 2017. mTORC2 signalling regulates M2 macrophage differentiation in response to helminth infection and adaptive thermogenesis. Nat. Commun. 8, 14208.
Hirota, N., Martin, J.G., 2013. Mechanisms of airway remodeling. Chest 144, 1026–1032.
Hogg, J.C., Chu, F., Utokaparch, S., 2004. The nature of small-airway obstruction in chronic obstructive pulmonary disease. N. Engl. J. Med. 350, 2645–2653.
Huang, S.C., Smith, A.M., Everts, B., Colonna, M., Pearce, E.L., Schilling, J.D., Pearce, E. J., 2016. Metabolic reprogramming mediated by the mTORC2-IRF4 signaling axis is essential for macrophage alternative activation. Immunity 45, 817–830.
Jones, R.L., Noble, P.B., Elliot, J.G., James, A.L., 2016. Airway remodelling in COPD: it's not asthma! Respirology 21, 1347-1356.
Kardas, G., Daszyńska-Kardas, A., Marynowski, M., Brząkalska, O., Kuna, P., Panek, M., 2020. Role of platelet-derived growth factor (PDGF) in asthma as an immunoregulatory factor mediating airway remodeling and possible pharmacological target. Front. Pharmacol. 11, 47.
Lai, T., Tian, B., Cao, C., Hu, Y., Zhou, J., Wang, Y., Wu, Y., Li, Z., Xu, X., Zhang, M., Xu, F., Cao, Y., Chen, M., Wu, D., Wu, B., Dong, C., Li, W., Ying, S., Chen, Z., Shen, H., 2018. HDAC2 suppresses IL17A-mediated airway remodeling in human and experimental modeling of COPD. Chest 153, 863–875.
Li, J., Yang, L., Yao, Q., Li, Y., Tian, Y., Li, S., Jiang, S., Wang, Y., Li, X., Guo, Z., 2014. Effects and mechanism of bufei yishen formula in a rat chronic obstructive pulmonary disease model. Evid. Based Complement. Alternat. Med., 381976, 2014.
Li, J.S., Liu, X.F., Dong, H.R., Zheng, W.C., Feng, S.X., Tian, Y.G., Zhao, P., Ma, J.D., Ren, Z.X., Xie, Y., 2020. Effective-constituent compatibility-based analysis of Bufei Yishen formula, a traditional herbal compound as an effective treatment for chronic obstructive pulmonary disease. J. Integr. Med. 18, 351–362.
Li, S.Y., Li, J.S., Wang, M.H., Xie, Y., Yu, X.Q., Sun, Z.K., Ma, L.J., Zhang, W., Zhang, H.L., Cao, F., Pan, Y.C., 2012a. Effects of comprehensive therapy based on traditional Chinese medicine patterns in stable chronic obs tructive pulmonary disease: a four-center, open-label, randomized, controlled study. BMC Complement. Altern. Med. 12, 197.
Li, Y., Li, S.Y., Li, J.S., Deng, L., Tian, Y.G., Jiang, S.L., Wang, Y., Wang, Y.Y., 2012b. A rat model for stable chronic obstructive pulmonary disease induced by cigarette smoke inhalation and repetitive bacterial infection. Biol. Pharm. Bull. 35 (10), 1752–1760.
Liao, X., Sharma, N., Kapadia, F., Zhou, G., Lu, Y., Hong, H., Paruchuri, K., Mahabeleshwar, G.H., Dalmas, E., Venteclef, N., Flask, C.A., Kim, J., Doreian, B.W., Lu, K.Q., Kaestner, K.H., Hamik, A., Clément, K., Jain, M.K., 2011. Krüppel-like factor 4 regulates macrophage polarization. J. Clin. Invest. 121, 2736–2749.
Lin, S.C., Chou, H.C., Chen, C.M., Chiang, B.L., 2019. Anti-thymic stromal lymphopoietin antibody suppresses airway remodeling in asthma through reduction of MMP and CTGF. Pediatr. Res. 86, 181–187.
Linke, M., Fritsch, S.D., Sukhbaatar, N., Hengstschläger, M., Weichhart, T, mTORC1 and mTORC2 as regulators of cell metabolism in immunity, 2017. mTORC1 and mTORC2 as regulators of cell metabolism in immunity. FEBS Lett. 591, 3089–3103.
Lortet-Tieulent, J., Soerjomataram, I., López-Campos, J.L., Ancochea, J., Coebergh, J.W., Soriano, J.B., 2019. International trends in COPD mortality, 1995-2017. Eur. Respir. J. 54.
Murray, L.A., Chen, Q., Kramer, M.S., Hesson, D.P., Argentieri, R.L., Peng, X., Gulati, M., Homer, R.J., Russell, T., van Rooijen, N., Elias, J.A., Hogaboam, C.M., Herzog, E.L., 2011. TGF-beta driven lung fibrosis is macrophage dependent and blocked by Serum amyloid P. Int. J. Biochem. Cell Biol. 43, 154–162.
Parisi, L., Gini, E., Baci, D., Tremolati, M., Fanuli, M., Bassani, B., Farronato, G., Bruno, A., Mortara, L., 2018. Macrophage polarization in chronic inflammatory diseases: killers or builders? J. Immunol. Res. 2018, 8917804.
Shaykhiev, R., Krause, A., Salit, J., Strulovici-Barel, Y., Harvey, B.G., O'Connor, T.P., Crystal, R.G., 2009. Smoking-dependent reprogramming of alveolar macrophage polarization: implication for pathogenesis of chronic obstructive pulmonary disease. J. Immunol. 183, 2867–2883.
Smyth, D.C., Kerr, C., Li, Y., Tang, D., Richards, C.D., 2008. Oncostatin M induction of eotaxin-1 expression requires the convergence of PI3′K and ERK1/2 MAPK signal transduction pathways. Cell. Signal. 20, 1142–1150.
Tashkin, D.P., Celli, B., Senn, S., Burkhart, D., Kesten, S., Menjoge, S., Decramer, M., 2008. A 4-year trial of tiotropium in chronic obstructive pulmonary disease. N. Engl. J. Med. 359, 1543–1554.
Vlahos, R., Bozinovski, S., 2014. Role of alveolar macrophages in chronic obstructive pulmonary disease. Front. Immunol. 5, 435.
Xue, J., Sharma, V., Hsieh, M.H., Chawla, A., Murali, R., Pandol, S.J., Habtezion, A., 2015. Alternatively activated macrophages promote pancreatic fibrosis in chronic pancreatitis. Nat. Commun. 6, 7158.
Yamasaki, K., Eeden, S.F.V., 2018. Lung macrophage phenotypes and functional responses: role in the pathogenesis of COPD. Int. J. Mol. Sci. 19.
Zeng, H., Cohen, S., Guy, C., Shrestha, S., Neale, G., Brown, S.A., Cloer, C., Kishton, R.J., Gao, X., Youngblood, B., Do, M., Li, M.O., Locasale, J.W., Rathmell, J.C., Chi, H., 2016. mTORC1 and mTORC2 kinase signaling and glucose metabolism drive follicular helper T cell differentiation. Immunity 45, 540–554.